Modeling Influence of Sediment Heterogeneity on Nutrient Cycling in Streambeds

AGU100 ADVANCING EARTH AND SPACE SCIENCE

Water Resources Research

RESEARCH ARTICLE
10.1029/2018WR024221

Key Points:
- Role of physical and chemical heterogeneity of streambed sediments on denitrification is numerically investigated
- Silt sediments promote denitrification since they experience longer residence times and are source of dissolved organic carbon
- Streambeds with mixture of sand and silt have high capacity to remove nitrate despite moderate permeabilities

Correspondence to:
E. Pescimoro,
eugenio.pescimoro@gmail.com

Citation:
Pescimoro, E., Boano, F., Sawyer, A. H., & Soltanian, M. R. (2019). Modeling influence of sediment heterogeneity on nutrient cycling in streambeds. *Water Resources Research*, *55*, 4082–4095. https://doi.org/10.1029/2018WR024221

Received 7 OCT 2018
Accepted 20 APR 2019
Accepted article online 30 APR 2019
Published online 15 MAY 2019

This article was corrected on 15 MAY 2020. See the end of the full text for details.

Modeling Influence of Sediment Heterogeneity on Nutrient Cycling in Streambeds

Eugenio Pescimoro[1,2], Fulvio Boano[1], Audrey H. Sawyer[3], and Mohamad Reza Soltanian[4]

[1]Department of Environment, Land, and Infrastructure Engineering, Politecnico di Torino, Turin, Italy, [2]School of Mathematical Sciences, The University of Nottingham, Nottingham, UK, [3]School of Earth Sciences, The Ohio State University, Columbus, OH, USA, [4]Departments of Geology and Environmental Engineering, University of Cincinnati, Cincinnati, OH, USA

Abstract Rivers and their hyporheic zones play an important role in nutrient cycling. The fate of dissolved inorganic nitrogen is governed by reactions that occur in the water column and streambed sediments. Sediments are heterogeneous both in term of physical (e.g., hydraulic conductivity) and chemical (e.g., organic carbon content) properties, which influence water residence times and biogeochemical reactions. Yet few modeling studies have explored the effects of both physical and chemical heterogeneity on nutrient transport in the hyporheic zone. In this study, we simulated hyporheic exchange in physically and chemically heterogeneous sediments with binary distributions of sand and silt in a low-gradient meandering river. We analyzed the impact of different silt/sand patterns on dissolved organic carbon, oxygen, nitrate, and ammonium. Our results show that streambeds with a higher volume proportion of silt exhibit lower hyporheic exchange rates but more efficient nitrate removal along flow paths compared to predominantly sandy streambeds. The implication is that hyporheic zones with a mixture of inorganic sands and organic silts have a high capacity to remove nitrate, despite their moderate permeabilities.

Plain Language Summary With the advent of intensive cultivation and livestock farms, nutrient contamination has increased in streams. Microbial communities in streambeds reduce nitrate, effectively removing it from streams. However, quantifying this removal is difficult because it is influenced by many spatially variable factors, among which sediment type plays an important role. Streambeds can contain both sandy and silty sediments distributed in complex patterns. The present study employs computer simulations to analyze how nitrate is removed in a mixture of different streambed sediments.

1. Introduction

Nitrate is a widespread contaminant that contributes to eutrophication of both inland and coastal waters (Nixon, 1995; Vitousek et al., 1997). Small streams and rivers play an important role in nitrate retention through biological uptake and removal through denitrification (Alexander et al., 2000; Seitzinger et al., 2002). Much of the nitrate removal occurs in anoxic areas or microsites near stream channels where surface water and groundwater mix (hyporheic zones) (Harvey et al., 2013; Hedin et al., 1998; Triska et al., 1993). In order for the hyporheic zone to effectively remove nitrate from stream water, the flux of nitrate to the streambed must be high, a source of labile dissolved organic carbon (DOC) must be available (Hedin et al., 1998; Zarnetske et al., 2011b), and the residence time must be long enough for dissolved oxygen to be consumed (Marzadri et al., 2012; Sawyer, 2015; Zarnetske et al., 2011a). All these conditions are influenced by sediment properties (Puckett et al., 2008). Sediment permeability influences the delivery rate of nitrate from stream water to the hyporheic zone and residence time of stream water within the hyporheic zone. Organic matter in sediments provides a local source of DOC for denitrification (Baker & Vervier, 2004).

Numerical models have increasingly been used to quantify denitrification within idealized hyporheic zones across a variety of scales (Briggs et al., 2015; Gomez-Velez et al., 2015; Sawyer, 2015; Trauth et al., 2014). Most of these models have focused on the role of channel morphology and stream hydrodynamics in controlling reactant supply from the stream and residence times in the river bed (Bardini et al., 2012; Kessler et al., 2012; Trauth & Fleckenstein, 2017). Models generally reveal that downwelling zones are associated with thicker aerobic zones and deeper denitrification fronts (Kessler et al., 2012; Marzadri et al., 2012). As hyporheic exchange increases, the aerobic zone expands in a predictable way with the

Damköhler number (the ratio of the characteristic hyporheic residence time to the oxygen consumption time). The efficiency of nitrate removal along hyporheic flow paths increases and then peaks with greater hyporheic exchange rates and shorter residence times (Marzadri et al., 2012). Many models of hyporheic denitrification lack a sediment source of DOC, so the supply of DOC from surface water or groundwater also controls nitrate removal (Bardini et al., 2012; Hester et al., 2014). Most models assume homogeneous sediment properties. Results are therefore representative of hyporheic zones with relatively uniform sediment composition, where redox conditions are primarily vertically stratified, but reaction fronts undulate beneath bedforms.

In field observations of more heterogeneous streambeds, redox conditions vary strongly over small spatial scales associated with changes in lithology or sediment composition (Krause et al., 2013; Lewandowski & Nutzmann, 2010; Puckett et al., 2008). Complex reaction fronts can occur that are influenced by both bedform morphology and streambed sediment composition. For example, Claret et al. (1997) showed that patches of fine sediments in gravel bars contained more total organic matter and bacteria and had lower concentrations of dissolved oxygen and nitrate. Krause et al. (2013) observed a depletion of dissolved oxygen and nitrate near peat and clay lenses. These studies suggest that finer, organic-rich sediments are sites of efficient respiration because they are relatively immobile zones with a local source of DOC. While some hyporheic studies have sought to represent this sediment heterogeneity, many have only considered the associated heterogeneity in permeability and not DOC supply (Bardini et al., 2013; Gomez-Velez et al., 2014; Pryshlak et al., 2015; Zhou et al., 2014). Permeability is a key parameter because it varies by orders of magnitude in riverbed deposits (Calver, 2001). Residence times are significantly longer within impermeable zones, allowing more time for chemical processing. However, few studies have explored the effects of heterogeneity in chemical parameters such as organic matter content. In natural streambed sediments and floodplain aquifers, organic matter content varies widely and has been shown to influence potential respiration rates (Arango et al., 2007; Puckett et al., 2002; Stelzer et al., 2011; Stelzer et al., 2014). Models that lack a local and heterogeneous source of organic carbon may not represent observed trends in respiration.

Given that the supply of organic carbon often limits denitrification in the subsurface, it is important to understand the effect of heterogeneity in both permeability and local DOC sources on nitrate removal in the subsurface (Bradley et al., 1992; Korom, 1992; Starr & Gillham, 1993). Fine-grained organic matter can locally relieve a DOC limitation on denitrification. It also increases the time available for denitrification by slowing the advection process. The structure of organic-rich sediments may be particularly important (Sawyer, 2015), since DOC is supplied from relatively immobile zones, while terminal electron acceptors (dissolved oxygen and nitrate) are supplied from relatively mobile zones connected to the channel. Our goal was to test the effects of this heterogeneity on hyporheic zone denitrification using a numerical sensitivity study based on a synthetic, heterogeneous hyporheic zone and floodplain aquifer. In all simulations, we prescribed two lithologies that are internally uniform: a low-permeability silt with more organic matter and a high-permeability sand with negligible organic matter. We maintained the same channel morphology but varied the structure of sand and organic-rich silt. Our results showed that in heterogeneous sediments, the nontrivial interactions between hyporheic exchange flux, residence times, and organic carbon availability have different effects on carbon, oxygen, and nitrogen transported in the hyporheic zone and control the overall rate of nutrient transformation in streambed sediments.

2. Methods

A three-dimensional (3-D) domain was created to simulate hyporheic flow through a single meander representative of those found in low-gradient meandering streams (Figure 1). The riverbed planform and bathymetric profiles are both described by the same sinusoidal functions that are reported in Boano et al. (2010). The channel width was 30 m, channel depth was varying between 0.8 and 1.2 m, sinuosity was low (1.03), and average down-valley slope was 2.06×10^{-3} [−]. This idealized channel geometry allowed us to compute the spatial distribution of hydraulic head on the sediment-water interface, which represented the upper boundary condition for the groundwater flow model. The 3-D subsurface domain was 471-m long, 140-m wide, and 3-m tall (Figure 1). We chose 3 m as vertical dimension of the model because it was found to be enough to minimize the influence of the lower boundary on flow and particle tracking. The influence of streambed topography on hyporheic exchange is indirect, that is, topography induces variations in surface

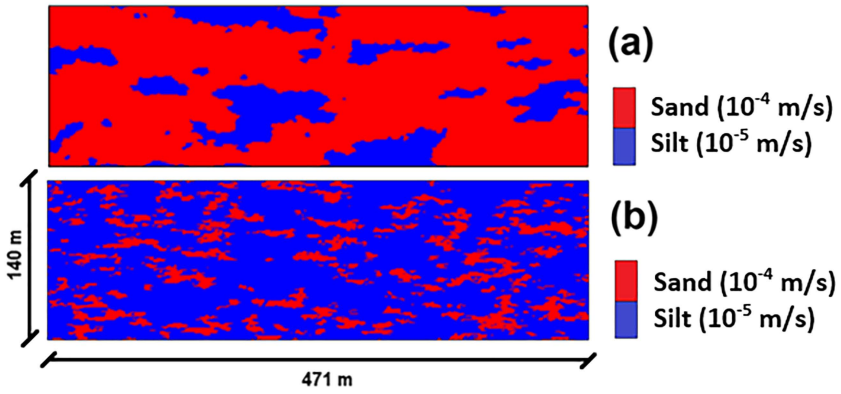

Figure 1. (a) Top view of elevation in the channel and surrounding floodplain (b) Transverse cross section.

water elevation, which drive hyporheic exchange through the streambed surface. Indeed, the water exchange we considered is not driven by flow separation at the downstream side of bedforms (Elliott & Brooks, 1997), which is typical of small dunes and ripples. Instead, the head distribution that drives exchange is here due to the influence of large-scale bars and meanders on the elevation of the stream water surface. Therefore, streambed topography was not explicitly represented in the shape of the domain (the top face of the model is planar, but a spatially varying head is prescribed to it), similar to many hyporheic models (Elliott & Brooks, 1997).

The 3-D steady state groundwater flow equation was solved using the finite difference approach in MODFLOW (Harbaugh & McDonald, 1996). The model bottom and lateral valley sides were represented as no-flow boundaries. The top boundary condition for hydraulic head within the channel was derived from the solution of a mathematical model that links Exner's equation to shallow water equations (Boano et al., 2010). The linear solution for the hydraulic head in the stream and for the bed topography was provided by the recent theory of Zolezzi and Seminara (2001). The idealized channel geometry and hydraulic river head were the same as in Boano et al. (2010). In order to determine the upper boundary condition in the floodplain, we solved for the hydraulic head in a two-dimensional (2-D) groundwater flow model using only the upper layer of cells. In this 2-D model, we prescribed values of hydraulic head along the channel edges and no-flow boundaries along valley edges as in the 3-D model. We also assumed that hydraulic head values along the upstream and downstream edges of the model were uniform and equal to the hydraulic head values at the left and right sides of the channel banks. The resulting 2-D solution for hydraulic head can be thought of as representing the water table elevation under neutral stream flow conditions (no net groundwater inflow or outflow along the reach). We applied this hydraulic head value as the upper boundary condition in the floodplain zones of 3-D models. No flow conditions were imposed over bottom and lateral boundaries. Finally, hydraulic head along the upstream and downstream faces of the model was held constant vertically, to yield no vertical component of flow across these faces.

Table 1
Indicator Correlation Length, Variance of Log Conductivity, and Correlation Length of Conductivity for Each Silt to Sand Ratio in the Downstream Direction

Silt to sand ratio	Silt volume proportion	Sand volume proportion	Mean length for sand (m)	Variance	Correlation length (m)
0.25	0.2	0.8	120	0.85	24
0.5	0.33	0.67	60	1.17	20
1	0.5	0.5	30	1.3	15
2	0.67	0.33	15	1.17	10
4	0.8	0.2	12.5	0.85	6

The domain was discretized with 1 m by 1 m cells with a height of 0.25 m, for a total number of 471 columns, 140 rows, and 12 layers. The cell height is small compared with mean length for silt and sand facies in vertical direction (minimum 1 m), and therefore, the model resolves vertical flow at the length scale of facies transitions.

There is a lack of comprehensive field observations on physical characteristics of sediments (mean lengths and volume proportions) in stream beds, but Kennedy et al. (2009) have shown that this heterogeneity can exert a strong control on nitrogen transport. Similar to Pryshlak et al. (2015), we chose to investigate the effects of large-scale variations in a binary distribution of sand and silt facies on hyporheic flow and transport. In our simulations of heterogeneity, we used mean lengths for the silt facies of

30 m in the downstream direction, 10 m in the cross-stream direction, and 1 m in the vertical direction. Using the fixed length for silt facies, we created sets of different heterogeneity simulations with silt/sand ratios of 0.25, 0.5, 1, 2, and 4. For example, a silt/sand ratio of 0.25 simply means silt and sand have volume proportions of 20% and 80%, respectively, in the computed domain. The five ratios we chose have been observed in a range of fluvial deposits (Engdahl et al., 2010; Ritzi et al., 2004; Weissmann et al., 1999; Weissmann & Fogg, 1999) but are not derived from any one field study.

We assigned heterogeneity in lithology and hydraulic conductivity using two steps. First, we represented spatial distribution of strata types (silt or sand). Second, we populated each cell with a hydraulic conductivity value for each strata type. Following the example of Pryshlak et al. (2015), we used a Markov Chain model and indicator simulation with quenching in Transition PRObability GeoStatistical software (TPROGS) (Carle, 1999) in order to simulate the structure of silt occurring within sand (Zhou et al., 2014). We used sand as a background strata. The Markov Chain model represents the length of silt strata in each direction using a transition probability structure having transition rate of $-1/L$, where L is the mean length (Soltanian et al., 2015a, 2015b). The quenching step helps to guarantee that the volume proportions for each strata type are honored.

In the second step, we assigned different hydraulic conductivity values (K) to sand and silt strata types across all grid cells ($K_{\text{silt}} = 10^{-5}$ m/s,$K_{\text{sand}} = 10^{-4}$ m/s; Domenico & Schwartz, 1990). Heterogeneity in organic carbon content of sand and silt facies was also considered, as described below in section 3. Specifically, a sediment source of dissolved organic carbon was applied in the silt facies but not the sand facies.

Pryshlak et al. (2015) showed that statistics of hyporheic metrics, such as residence time ranges, become stable for a given silt/sand ratio when the number of simulations is higher than 20. Thus, here we chose 30 simulations for each silt/sand ratio. Each simulation represents a unique arrangement of sand and silt facies. It is known that the volume proportion controls facies connectivity (Harter, 2005). In a binary system, such the one here, the mean length is also an indicator for connectivity due to its relation to volume proportion (Guin & Ritzi, 2008). Thus, given a fixed mean length of silt facies, sand facies connectivity decreases as silt/sand ratio increases (Table 1). Note that the correlation lengths of the sand facies (Table 1) and silt facies (30 m) specified in TPROGS are mathematical representations of heterogeneity that embody the relative proportions of sand and silt and mean lengths of the sand and silt bodies (Soltanian, Ritzi, Dai, et al., 2015; Soltanian et al., 2017). The correlation lengths should not be expected to exactly resemble the typical length of each strata type. Examples of K fields resulting from TPROGS are showed in Figure 2.

MODPATH (Pollock, 2012) was used to determine flow paths and residence times of 14,591 particles that were released at the streambed surface. Each cell of the streambed was set as the starting position for one particle, thus the overall number of particles. The subset of particles located in downwelling zones that entered the domain was used to determine the flux-weighted residence time distribution for each simulation.

3. Biogeochemical Model

Reactive transport along flow paths was treated with the streamtube approach. This approach does not account for diffusion as MODPATH computes particle tracking only by considering the advective term of the flow. Aerobic respiration, nitrification, and denitrification are respectively expressed by reactions (1) to (3):

$$\{\text{DOC} + \text{O}_2 \rightarrow \text{CO}_2 + \text{H}_2\text{O} \tag{1}$$

$$\{\text{DOC} + \text{NO}_3 \rightarrow \text{CO}_2 + \text{N}_2 + \text{H}_2\text{O} \tag{2}$$

$$\{\text{NH}_4 + 2\text{O}_2 \rightarrow \text{NO}_3 + 2\text{H} + \text{H}_2\text{O} \tag{3}$$

We used the residence times along flow pathways in order to solve the transient ordinary differential equations below for each species concentration (equations (4)–(7)) using the explicit *ode23* solver implemented in Matlab (Shampine & Reichelt, 1997). We mapped the resulting concentrations back to the flow pathways, following the approach by Frei et al. (2012). Mass conservation equations are solved for four chemical species of dissolved oxygen (O_2), ammonium (NH_4^+), nitrate (NO_3^-), and dissolved organic carbon (DOC):

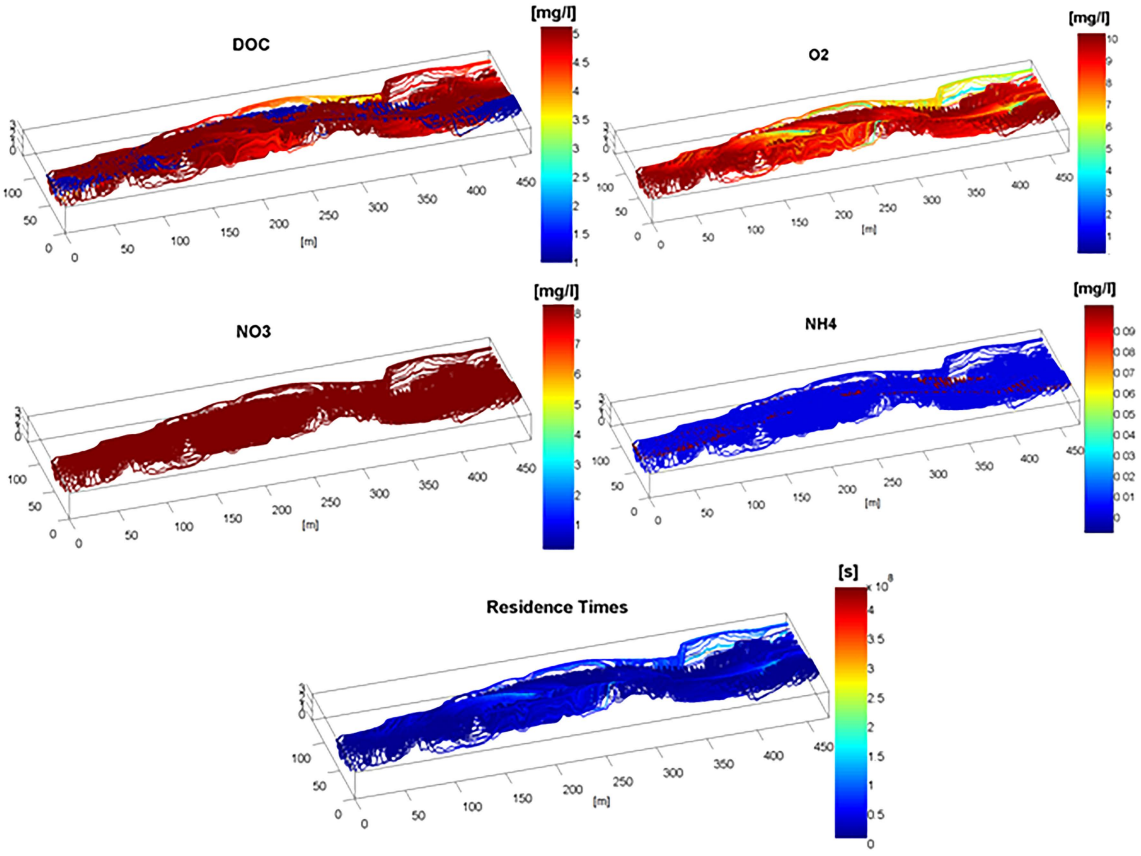

Figure 2. Examples of conductivity fields from simulations with opposite ratio: (a) silt/sand = 0.25 (b) silt/sand = 4.

$$\begin{cases}\frac{dC_{DOC}}{dt} = -K_{DOC}C_{DOC}(f_1+f_2) + \delta\frac{\rho}{\phi}\alpha(POC - K_dC_{DOC}) \end{cases} \quad (4)$$

$$\begin{cases}\frac{dC_{O2}}{dt} = -a_{O2}K_{DOC}C_{DOC}f_1 - b_{O2}K_{NITR}C_{NH4}C_{O2} \end{cases} \quad (5)$$

$$\begin{cases}\frac{dC_{NO3}}{dt} = -a_{NO3}K_{DOC}C_{DOC}f_2 + b_{NO3}K_{NITR}C_{NH4}C_{O2} \end{cases} \quad (6)$$

$$\begin{cases}\frac{dC_{NH4}}{dt} = -b_{NH4}K_{NITR}C_{NH4}C_{O2} \end{cases} \quad (7)$$

where C_{DOC},C_{O2},C_{NO3},and C_{NH4} represent concentrations of the dissolved species, a_{O2},b_{O2},a_{NO3},b_{NO3}, and b_{NH4} are stoichiometric coefficients (i.e., ratios between moles of transferred electrons per mole of oxidized compound and moles of electrons per mole of reduced compound), K_{DOC} and K_{NITR} are first- and second-order kinetic coefficients for heterotrophic and autotrophic reactions, respectively, K_d is the distribution coefficient of organic carbon between sediment and water, α is the mass transfer coefficient for organic carbon exchange between sediment and water, ρ and ϕ represents soil density and porosity, and δ is an index that is equal to 1 or 0 if the particle is in a silt or sand cell, respectively. The use of δ differentiates the chemical properties of silt facies (rich in particulate organic carbon [POC] and acting as a potential source of DOC) from those of sand units that are primarily composed of mineral elements with negligible POC content (no source of DOC).

The variables f_1 and f_2 determine concentration-dependent reaction kinetics for aerobic and anaerobic respiration. When the concentration of oxygen is greater than the limit C_{O2lim}, f_1 equals 1, and the rate of aerobic respiration in equations (4) and (5) becomes independent of oxygen concentration. When oxygen concentration is less than C_{O2lim}, f_1 becomes linearly proportional to C_{O2}.

Table 2
List of Parameter Values Adopted in the Biogeochemical Model

Parameter	Value	Source
a_{O2}	1	Stoichiometric balances
b_{O2}	2	Stoichiometric balances
a_{NO3}	0.8	Stoichiometric balances
b_{NO3}	1	Stoichiometric balances
b_{NH4}	1	Stoichiometric balances
K_{DOC}	10^{-7} (s^{-1})	Hunter et al. (1998)
K_{nitr}	5×10^{-6} (L/(mg · s))	Hunter et al. (1998)
α	10^{-9} (s^{-1})	Gu et al. (2007)
POC	0.01 (mg/mg)	Peterson and Hayden (2018)
K_d	0.002 (L/mg)	Gu et al. (2007)
Φ	0.25 (L/L)	This work
ρ	2,237 (kg/m^3)	This work
C_{O2lim}	1 (mg/L)	Bardini et al. (2012)
C_{NO3lim}	5 (mg/L)	Bardini et al. (2012)

$$f_1 = \begin{cases} 0 & \text{if} \quad C_{O2} > C_{O2\,lim} \\ \dfrac{C_{O2}}{C_{O2\,lim}} & \text{if} \quad C_{O2} < C_{O2\,lim} \end{cases} \tag{8}$$

$$f_2 = (1-f_1)\begin{cases} 1 & \text{if} \quad C_{NO3} > C_{NO3\,lim} \\ \dfrac{C_{NO3}}{C_{NO3\,lim}} & \text{if} \quad C_{NO3} < C_{NO3\,lim} \end{cases} \tag{9}$$

It is important to consider that oxygen is a limiting factor for the rate of nitrification and that it also plays a relevant role in denitrification and in DOC consumption. With a structure similar to f_1, the purpose of f_2 is to regulate the rate of denitrification (see equation (6)). Nevertheless, f_2 includes the factor $(1 - f_1)$ in order to inhibit denitrification ($f_2 = 1 - f_1 = 0$) when oxygen concentration is higher than a given threshold; denitrification is allowed to occur when oxygen concentration drops and anaerobic conditions exist. The rate of denitrification, after passing a certain threshold, becomes linearly proportional to the concentration of the electron acceptor, which in this case is nitrate.

Possible sources of DOC in the model are stream water and sediment. Release of DOC from sediments is often represented as a reversible equilibrium process (e.g., associated with reversible sorption of DOC on organic matter; Gu et al., 2007). Because the sand facies is considered low in organic matter, the term for DOC production in the sediment is only included during time periods when the flow path passes through the organic-rich silt facies ($\delta = 1$). Due to the unique interaction of each flow path with sand and silt bodies, reactions along each path are unique, and equations (4)-(7) must be solved for each path in each simulation.

We specified initial concentrations at the downwelling zones characteristic of stream water with high nitrate concentration. Specifically, the nitrate concentration was 8 mg/L, ammonium was 0.1 mg/L, dissolved oxygen was 10 mg/L, and DOC was 1 mg/L (Warner et al., 2009). Values for other biogeochemical parameters are listed in Table 2. The value for K_{DOC} was chosen to represent natural organic matter with relatively low lability (Hunter et al., 1998) that degrades over typical residence times of the system. The variety of organic matter existing in nature covers a wide range of slightly different substances, leading to K_{DOC} values that

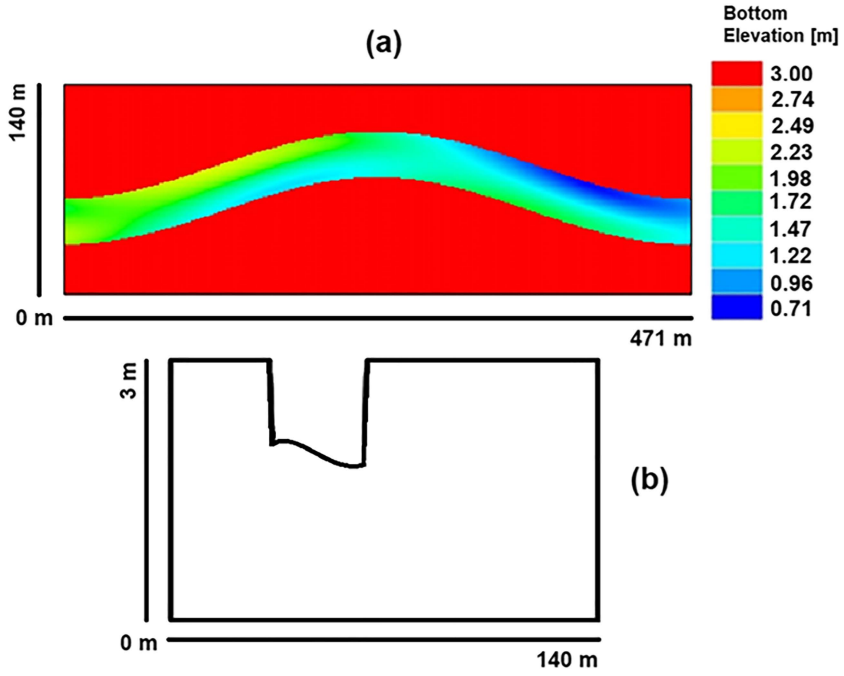

Figure 3. Concentration dynamics of dissolved organic carbon (DOC), oxygen, ammonium, and nitrate along a particle flow path (silt/sand = 1). The time spent in silt facies is denoted by shaded areas.

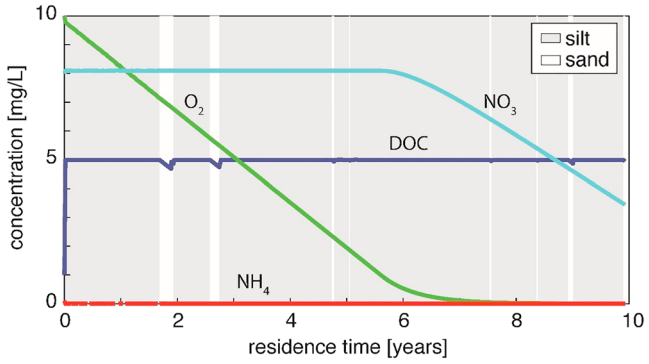

Figure 4. Flow paths for one simulation with silt/sand = 1. For NO_3^-, the uniform color is due to the fact that particle paths with variable concentration are hidden by the most superficial ones. DOC = dissolved organic carbon.

vary by ten magnitude orders from the most labile organic matter (K_{DOC} = 10^{-7}/year = 0.3/s) to the most refractory (K_{DOC} = 10^3/year= 10^{11}/s). In this low-gradient stream, residence times are long compared with high-gradient gravel streams, and we chose a value of K_{DOC} representative of more refractory DOC to ensure that modeled oxygen concentrations would span a range of high and low values in sand and silt, similar to observed oxygen concentrations from other parafluvial systems (Malard & Hervant, 1999). We neglected the influence of temperature on reaction kinetics, since the aim of the present work was that of analyzing the reactive behavior of hyporheic sediments in response to sediment properties.

4. Results

The combination of low permeability in a low-gradient meander resulted in long residence times over which nutrient concentrations evolve at different rates. An example of predicted nutrient dynamics along a single flow path is presented in Figure 3 for a simulation with silt/sand ratio of 1. As soon as water enters organic-rich silt sediments, the DOC concentration quickly equilibrates with soil POC (Figure 3). The resulting DOC equilibrium concentration (5 mg/l) remains constant along portions of the flow path in silt because the release of DOC occurs at much faster rates than DOC consumption by heterotrophic microorganisms. This is realistic at our length scale of investigation because the organic matter is slowly degradable and DOC replenishment is hence faster. DOC concentration decreases during flow through sand facies. For example, in the flow path shown in Figure 3, the limited amount of sand leads to minor drops in DOC concentration (<1 mg/l). Dissolved oxygen is progressively consumed, and the ensuing anaerobic conditions allow for denitrification to occur and progressively remove nitrate from pore water. For example, in the flow path shown in Figure 3, nitrate concentration declines after 6 years. Note that NH_4^+ is quickly converted to nitrate by nitrifying bacteria in aerobic conditions as soon as stream water enters hyporheic sediments. Due to its low concentration in stream water, NH_4^+ plays a minor role in nitrogen cycling in this study.

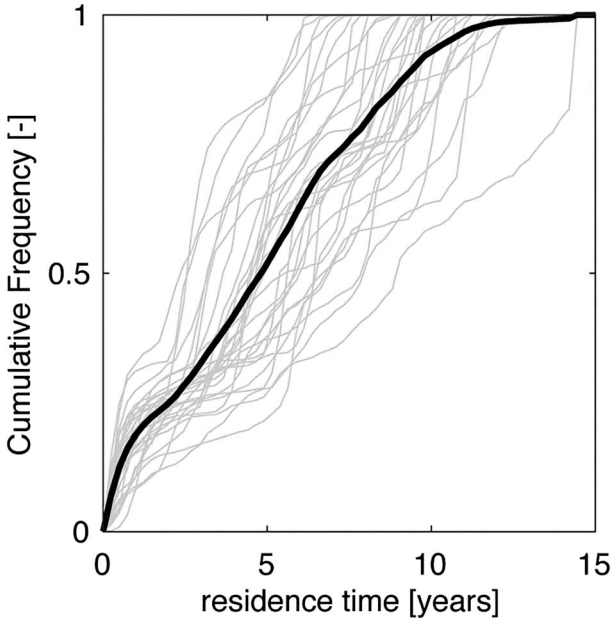

Figure 5. Residence time distributions for 30 simulations with silt/sand = 1. The gray lines denote individual simulations with the same silt/sand ratio, while the black line represents the ensemble average of the 30 simulations.

Residence times are a primary control for nutrient concentrations, and the net effect of hyporheic exchange on nutrient cycling will depend on the range of residence times experienced along different flow paths, as exemplified in Figure 4. For this reason, we chose kinetic parameters that would yield reaction rates on the order of our residence times. The results are presumably relevant for any system with similar Damkohler numbers.

The distribution of residence times (Figure 5) is influenced by the specific spatial arrangement of silt and sand facies. Even for a constant silt/sand ratio, the distribution of residence times varies across different simulations due to the positions of sand units within the riverbed and along flow paths (Pryshlak et al., 2015).

This variability in residence times due to sediment heterogeneity affects modeled nutrient concentrations (Figure 6). DOC concentrations exhibit some variability across simulations, with temporary decreases in concentration—when water flows through sand—followed by an abrupt recovery in silt. Terminal electron acceptors exhibit a relatively smooth decline as oxygen and then nitrate are consumed. The consistency in consumption of O_2 and NO_3^- concentrations among different simulations with the same silt/sand ratio arises because the rate of heterotrophic respiration primarily depends on available DOC concentrations (see equations (2) and (3)), which hover near the equilibrium value. This implies that concentrations of oxygen and nitrate are well described by the ensemble average of simulations with the same silt/sand ratio.

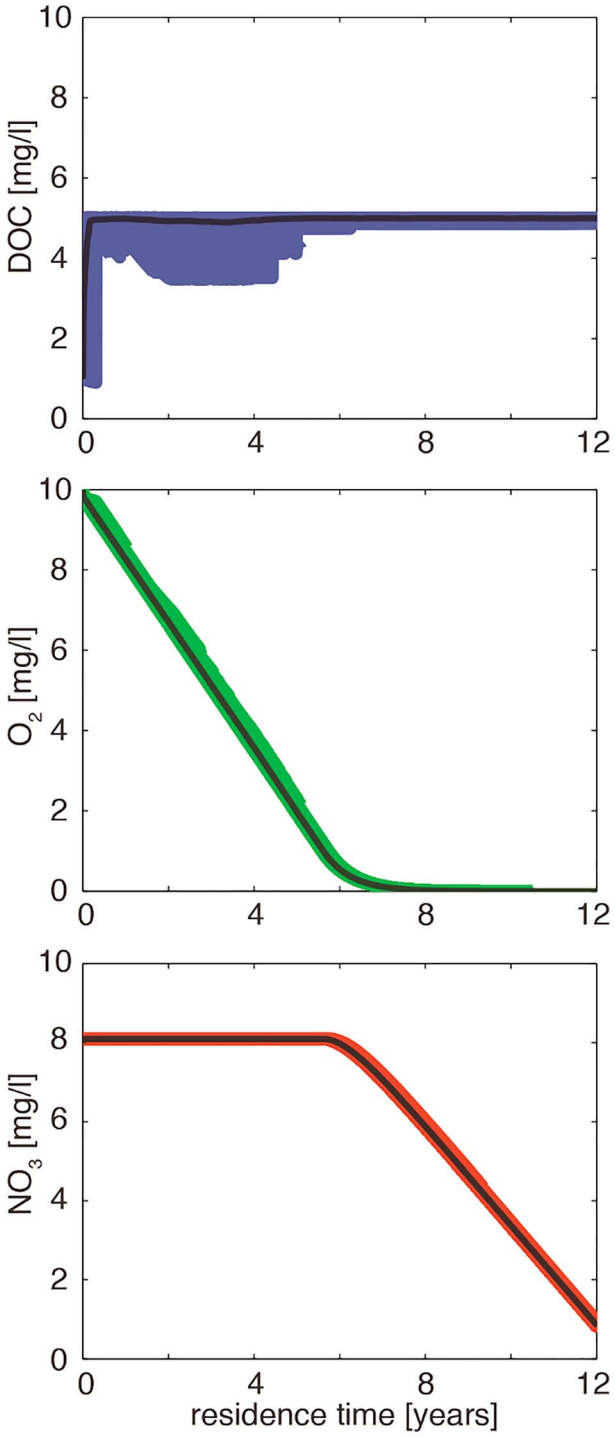

Figure 6. Profiles of dissolved organic carbon (DOC; blue), dissolved oxygen (green), and nitrate (red) for the 30 simulations with silt/sand = 1. Black line indicates average for the ensemble, colored lines represent single simulations, but they overlap. For this reason oxygen and nitrate look almost like a thicker line (especially for nitrate). NH_4^+ is not represented because of its extremely fast depletion.

Because ensemble averaged quantities effectively describe the relationship between concentrations and residence time for different simulations, they are hereinafter used to analyze the role of silt/sand ratio on nutrient transport and reaction. Residence times increase with the silt/sand ratio (Figure 7). Due to large volume fraction of sand for silt/sand ratios below 0.5, there are fully connected flow pathways in sand bodies that span the domain. Therefore, the residence time distributions for these cases are quite similar. For high silt/sand ratios, there are no fully connected flow pathways through sand bodies that span the domain. Therefore, flow paths experience longer residence times.

Due to variations in residence time distributions and the different organic content of silt and sand facies, nutrient dynamics are highly affected by subsurface heterogeneity. Figure 8 shows the ensemble averaged concentration profiles for two contrasting values of the silt/sand ratio of 4 and 0.25 residence times of 0 to 9 years. As silt/sand ratio increases, average DOC concentration approaches the equilibrium value more quickly. The other solutes exhibit a similar behavior regardless of the silt/sand ratio value. Notice that NH_4^+ is rapidly nitrified to NO_3^-, but due to its scarce presence in the considered system, it has little influence on the overall nitrogen balance. It should be emphasized that the overall variations of ensemble concentrations along flow paths derive from the combination of variations in both residence times (Figure 7) and reaction kinetics (Figure 8).

As expected, the analysis of the average exchange flux through the streambed reveals a progressive reduction in the exchange flux as the silt/sand ratio increases (Figure 9a). Variability among simulations also decreases with increasing silt/sand ratios (Figure 9a). For each nutrient, reaction efficiency can be calculated as the percentage of solute that is produced or consumed in the hyporheic zone relative to the influx. An efficiency of 0% indicates no net removal or production (solute outflow equals inflow), −100% indicates full removal, and 100% indicates a doubling of the solute outflow relative to inflow. Results show that exchanged water is always enriched in DOC, whose average concentration increases (up to a factor of 4) with increasing silt/sand ratio (Figure 9b). Oxygen decreases by 36.9% (silt/sand = 0.25) to 74.3% (silt/sand = 4) (Figure 9c). For nitrate, the behavior shifts from very slight net increase along flow paths (+0.8%) due to nitrification for silt/sand = 0.25 to strong net decrease (−31.8%) for higher silt fractions (Figure 9d). This shift with higher silt content is caused by lower oxygen availability, which favors denitrification and enhances removal of NO_3^-. Because ammonium is completely consumed by nitrification, its efficiency (not shown) is always equal to −100%.

Because the magnitude of the reaction efficiency increases with silt/sand ratio (Figures 9b–9d) but hyporheic fluxes decrease (Figure 9a), it is important to examine reaction rates for the streambed bioreactor in units of mass per time, where positive and negative values indicate production and consumption, respectively. On average, the net reaction rate of ammonium due to nitrification decreases with increasing silt/sand ratio (Figure 10d). Because all NH_4^+ delivered to the streambed is completely nitrified, the lower hyporheic flux leads to a lower NH_4^+ supply to the streambed and hence to lower reaction rates. Meanwhile, DOC and oxygen production or consumption rates remain roughly constant up to a silt/sand ratio of 0.5 then decline (Figures 10a and 10b). This behavior indicates that at low (<0.5) silt/sand ratio, the higher reaction efficiency induced by the increasingly higher POC

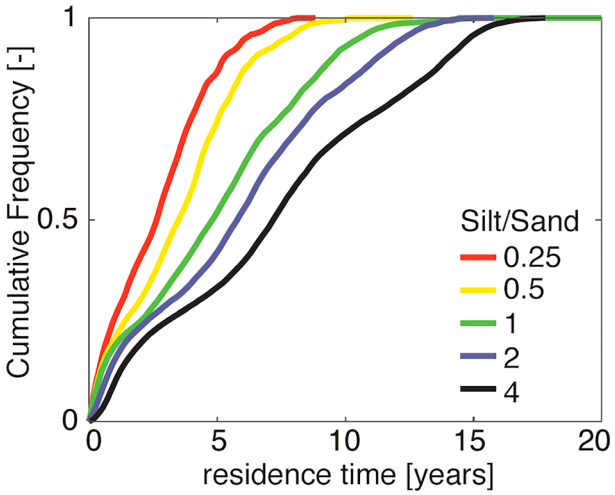

Figure 7. Variations of ensemble average of residence time distributions for different values of silt/sand ratio.

abundance compensates or dominates over the decrease in hyporheic flux in less permeable silty sediments. This behavior is reversed for silt/sand ratios larger than 0.5, for which the lower hyporheic fluxes dominate the reaction rates. Nitrate exhibits a different behavior, with a monotonic increase in consumption rates with higher silt/sand ratio (Figure 10c). We do not expect this trend to continue indefinitely, since a pure-silt bed would have an even lower hyporheic exchange rate that could limit the nitrate supply. At the opposite extreme, a pure-sand bed might have removal rates that are limited by short residence times as well as a lack of DOC supply from local organic matter. Apparently, the highest NO_3^- consumption efficiency (i.e., more negative values) occurs in siltier sediments, even though hyporheic exchange is lower. This implies that when the silt/sand ratio increases, a larger portion of the (decreasing) amount of NO_3^- supplied to the streambed is denitrified. Considerable variability exists among different simulations, as denoted by whiskers in Figure 10. This variability is particularly evident for oxygen and nitrate. For the case of DOC, the variability in reaction rates is highest for low values of silt/sand ratio. It also notable that oxygen removal efficiency trends toward 100% with more silt (Figure 9c) but the reaction rate will be limited by the supply rate with more silt (Figure 10c). That is also likely the reason of the local minimum in Figure 10b.

5. Discussion

Our study shows that siltier streambeds with less hyporheic exchange (Figure 9a) can remove as much or even more nitrate than sandier ones (Figure 10c). This result stems from the fact that the overall denitrification rate in our model streambed was reaction limited, while DOC, oxygen, and NH_4^+ showed an opposite flux-limited behavior (Figures 10a, 10b, and 10d). Interestingly, our results differ from those of the simulations of homogenous streambeds presented by Marzadri et al. (2012), who found that net nitrate removal increased with higher hydraulic conductivity (see their Figure 7a for streams with $NH_4^+ \ll NO_3^-$). Because in our study the range of Damköhler number values (defined as the ratio between the median residence time and the timescale for oxygen depletion, shown in Figure 7 and Figure 8b, respectively) is comparable with those of Marzadri et al. (2012), the difference in nitrate dynamics must be largely due to the influence of hydraulic heterogeneity. A possible explanation is that the variations in the shape of the residence time distribution among individual realizations of the K-field (Figure 5) are not fully represented by a single median residence time and affect the sensitivity of overall removal rate of NO_3^- to changes in average hydraulic conductivity. It should also be noted that we found cases of net nitrate production at low silt/sand ratio (Figure 10c), which were not predicted by Marzadri et al. (2012) for streams with similar stream water chemistry (in terms of NH_4^+/NO_3^- concentration ratio).

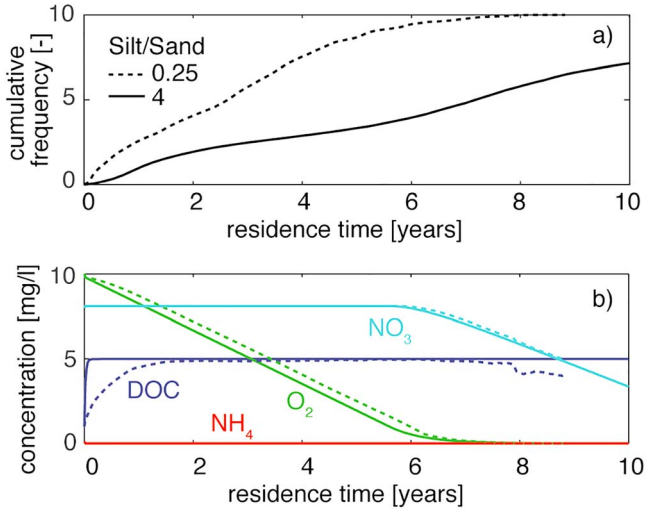

Figure 8. (a) Cumulative residence time for silt/sand ratio of 4 and 0.25 (b) ensemble averaged concentration profiles. DOC = dissolved organic carbon.

Another important feature of our models is the steep concentration gradients that develop between adjacent flow paths, particularly for oxygen and dissolved organic carbon (Figure 4). These concentration gradients develop along facies boundaries, where sand bodies remain more oxygen-rich and are depleted in DOC, while silt bodies become depleted in oxygen but enriched in DOC. Similar concentration gradients have been observed in streambeds due to the presence of peat or clay lenses (Krause et al., 2013), or beneath floodplain areas due to buried organic matter (Lewandowski & Nutzmann, 2010). These steep concentration gradients have been reproduced in other modeling studies with binary sedimentary facies (Sawyer, 2015), while smooth concentration distributions have been reported in the model study by Bardini et al. (2013). Beside our slightly higher degree of heterogeneity ($\sigma^2_{\ln(K)} = 0.85$–1.3, Table 1,

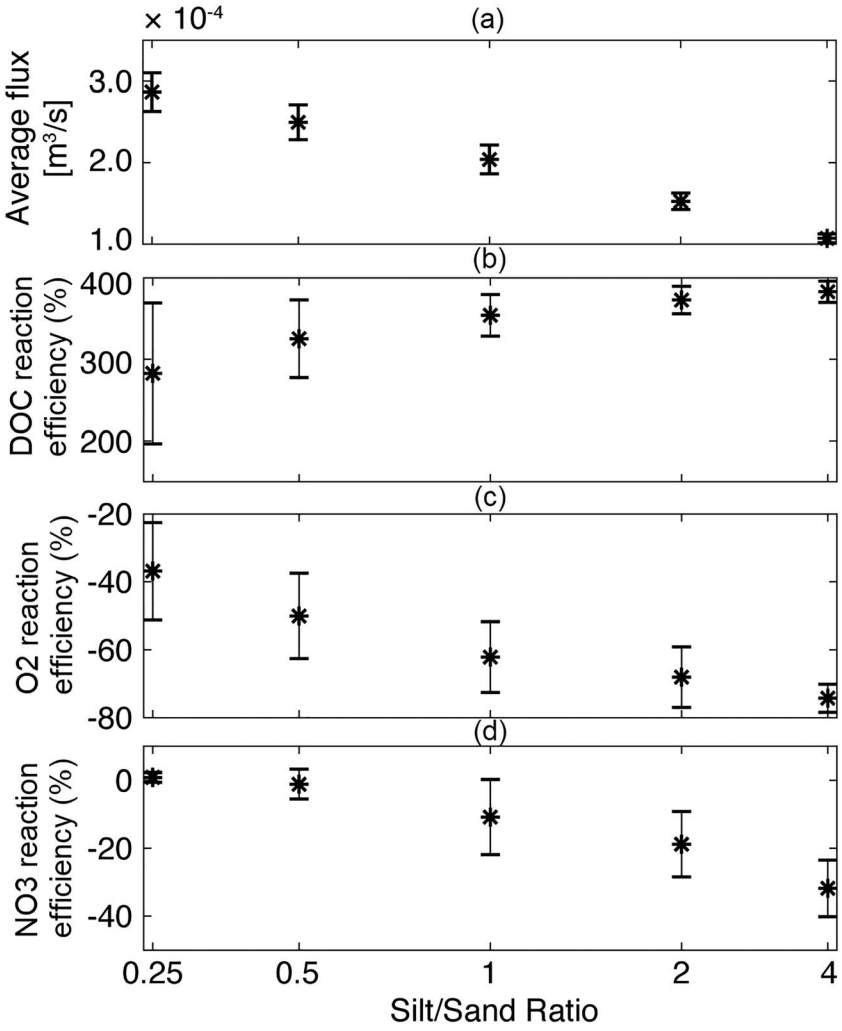

Figure 9. Average (markers) and standard deviations (whiskers) of (a) hyporheic exchange flux across the streambed and reaction efficiency for (b) dissolved organic carbon (DOC), (c) dissolved oxygen, and (d) nitrate. Positive and negative values of reaction efficiency indicate solute production and consumption, respectively.

compared to 0.15–0.94 for Bardini et al., 2013), the most relevant factor that explains the presence of sharp concentration gradients in our results is the supply of DOC from silt facies rich in particulate organic carbon. This feature, which was not included in the simulations of Bardini et al. (2013), results in high DOC concentrations (Figure 6a) that provide heterotrophic bacteria with the required carbon source for denitrification. Our study thus indicates the importance of considering heterogeneity in chemical composition of sediments when microbial reactions are expected to be limited by substrate availability. This effect can be even more important in highly heterogeneous sediments (e.g., Laube et al., 2018, with $\sigma^2_{\ln(K)}$ up to 6.7) comparted to our moderate degree of heterogeneity.

The present work did not consider the effect of solute dispersion (Kessler et al., 2012), which would cause mixing among different flow paths and further enhance supply of nutrients to otherwise depleted zones. Dispersive transport is expected to be important particularly at small spatial scales, as exemplified by studies of denitrification within low-permeability microzones where long residence times enhance development of anaerobic conditions (Briggs et al., 2015) and DOC release supports denitrification (Sawyer, 2015). Dispersive transport is commonly considered to be less important at larger (>1 m) scales as those considered in this study, even though it could still foster mixing of water with different chemistry at the boundaries between different facies (Hester et al., 2014). As for reaction and transport timescales in our models, it is true that reactions can occur much faster than those we are simulating (Zarnetske et al., 2011a). Note, however,

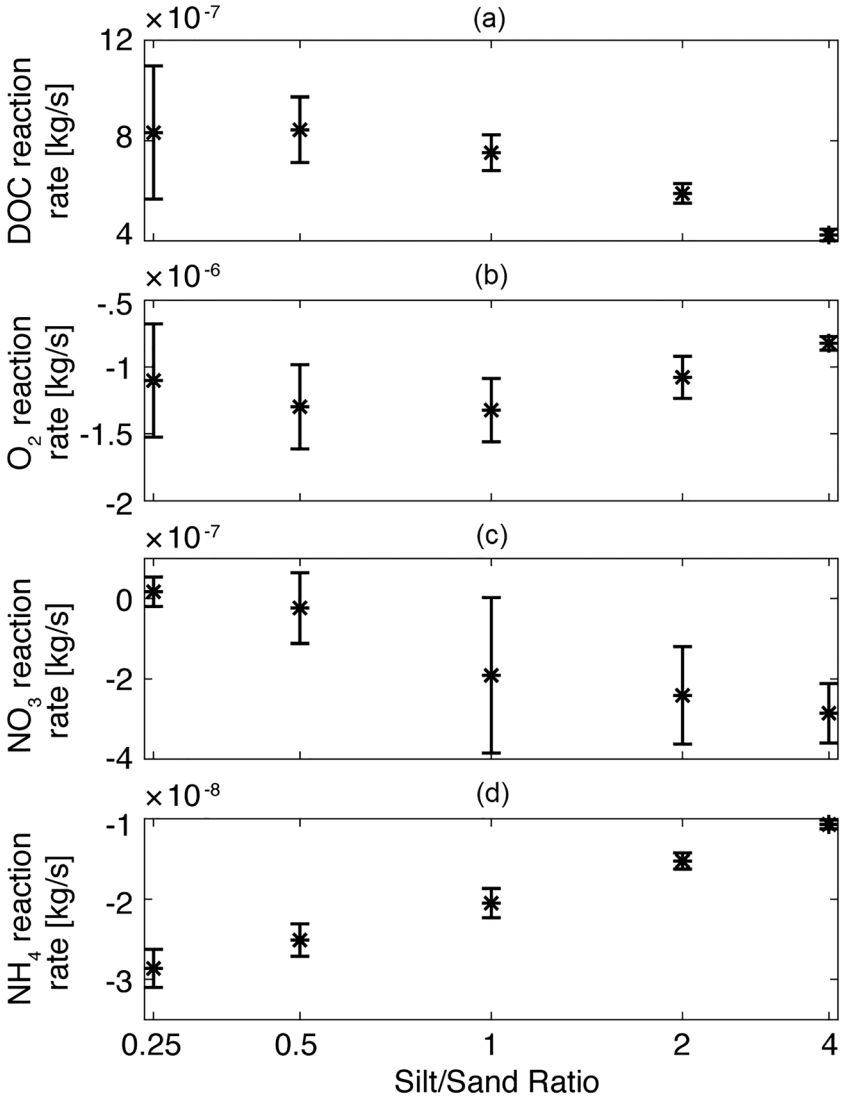

Figure 10. Average (markers) and standard deviations (whiskers) of net reaction rates for (a) dissolved organic carbon (DOC), (b) dissolved oxygen, (c) nitrate, and (d) ammonium. Fluxes and reaction rates are integrated across the streambed area which is 14,130 m^2.

that residence times in that system are also much shorter than ours; thus, we chose kinetics that would be on the order of our residence times. Finally, it should be recalled that shallow hyporheic exchange caused by streambed topography (Boano et al., 2014) was not included in the present model, which focuses on exchange at the length scale of the meander wavelength.

6. Conclusions

Heterogeneity in streambed sediment influences both hyporheic residence times through permeability and respiration rates through the supply of DOC from organic matter, but both effects are seldom included in hyporheic reactive transport models. In our numerical modeling study of a low-gradient, meandering river with sandy and silty sediment, we analyzed 150 binary arrangements of salt and silt across five different silt/sand ratios. For a given silt/sand ratio, nutrient concentrations are fairly consistent across different flow paths for a given residence time, regardless of whether that flow path has spent more time in silt or sand. Thus, residence time exerts a stronger control on removal than organic matter content for the parameters chosen in our study. However, different simulations with the same silt/sand ratio can have a range of residence time distributions driven by differences in permeability fields (e.g., location of sand bodies),

and these different residence time distributions affect average nutrient concentrations that return to the stream.

When sediments with different silt/sand ratios are compared, more substantial variations in hyporheic flux and residence times emerge. On one hand, exchange flux with the hyporheic zone decreases with increasing silt/sand ratio, reducing the supply of stream-borne nutrients to microbially active sediments. On the other hand, the progressive shift toward longer residence times with higher silt/sand ratio allows more time for nutrient removal along flow paths. The reduction of hyporheic exchange governs the total rate of aerobic respiration in the hyporheic zone. Aerobic respiration is maximized at intermediate silt/sand ratios, where residence times are sufficiently long but DOC supply from sediments is moderate. The total rate of denitrification tends to increase more consistently with silt/sand ratio. The streambed progressively switches from a slight source to a strong sink of nitrate. We emphasize that these results apply to low-gradient, silty to sandy streambeds and may differ for higher gradient, gravel streambeds. Our simulations emphasize the role of hydraulic and chemical heterogeneity and suggest the importance to refine as much as possible the description of heterogeneous sediment properties in modeling studies. Additional work is also needed to better characterize typical scales of heterogeneity in streambeds.

Acknowledgments
E. Pescimoro was supported by European funding from the Erasmus+ Internship Program. A. Sawyer was supported under NSF EAR 1752995. All the images and statements presented in this article are supported by archives of txt data obtained as a result of numerical simulations. MODFLOW input files, including hydraulic head and conductivity fields, are available on Zenodo at the following address: https://doi.org/10.5281/zenodo.2560349 and https://doi.org/10.5281/zenodo.2560349.

References

Alexander, R. B., Smith, R. A., & Schwarz, G. E. (2000). Effect of stream channel size on the delivery of nitrogen to the Gulf of Mexico. *Nature*, *403*(6771), 758–761. https://doi.org/10.1038/35001562

Arango, C. P., Tank, J. L., Schaller, J. L., Royer, T. V., Bernot, M. J., & David, M. B. (2007). Benthic organic carbon influences denitrification in streams with high nitrate concentration. *Freshwater Biology*, *52*, 1210–1222. https://doi.org/10.1111/j.1365-2427.2007.01758.x

Baker, M. A., & Vervier, P. (2004). Hydrological variability, organic matter supply and denitrification in the Garonne River ecosystem. *Freshwater Biology*, *49*(2), 181–190. https://doi.org/10.1046/j.1365-2426.2003.01175.x

Bardini, L., Boano, F., Cardenas, M. B., Revelli, R., & Ridolfi, L. (2012). Nutrient cycling in bedform induced hyporheic zones. *Geochimica et Cosmochimica Acta*, *84*, 47–61. https://doi.org/10.1016/j.gca.2012.01.025

Bardini, L., Boano, F., Cardenas, M. B., Sawyer, A. H., Revelli, R., & Ridolfi, L. (2013). Small-scale permeability heterogeneity has negligible effects on nutrient cycling in streambeds. *Geophysical Research Letters*, *40*, 1118–1122. https://doi.org/10.1002/grl.50224

Boano, F., Camporeale, C., & Revelli, R. (2010). A linear model for the coupled surface-subsurface flow in a meandering stream. *Water Resources Research*, *46*, W07535. https://doi.org/10.1029/2009WR008317

Boano, F., Harvey, J. W., Marion, A., Packman, A. I., Revelli, R., Ridolfi, L., & Wörman, A. (2014). Hyporheic flow and transport processes: Mechanisms, models, and biogeochemical implications. *Reviews of Geophysics*, *52*, 603–679. https://doi.org/10.1002/2012RG000417

Bradley, P. M., Fernandez, M. Jr., & Chapelle, F. H. (1992). Carbon limitation of denitrification rates in an anaerobic groundwater system. *Environmental Science & Technology*, *26*(12), 2377–2381. https://doi.org/10.1021/es00036a007

Briggs, M. A., Day-Lewis, F. D., Zarnetske, J. P., & Harvey, J. W. (2015). A physical explanation for the development of redox microzones in hyporheic flow. *Geophysical Research Letters*, *42*, 4402–4410. https://doi.org/10.1002/2015GL064200

Calver, A. (2001). Riverbed permeabilities: Information from pooled data. *Ground Water*, *39*(4), 546–553. https://doi.org/10.1111/j.1745-6584.2001.tb02343.x

Carle, S. F. (1999). *Transition probability geostatistical software, version 2.1*, 76 pp. Davis, California: University of California.

Claret, C., Marmonier, P., Boissier, J. M., Fontvieille, D., & Blanc, P. (1997). Nutrient transfer between parafluvial interstitial water and river water: Influence of gravel bar heterogeneity. *Freshwater Biology*, *37*(3), 657–670. https://doi.org/10.1046/j.1365-2427.1997.00193.x

Domenico, P. A., & Schwartz, F. W. (1990). *Physical and chemical hydrogeology* (824 pp.). New York: John Wiley. ISBN: 0 471 50744 X

Elliott, A. H., & Brooks, N. H. (1997). Transfer of nonsorbing solutes to a streambed with bed forms: Theory. *Water Resources Research*, *33*, 123–136. https://doi.org/10.1029/96WR02784

Engdahl, N. B., Vogler, E. T., & Weissmann, G. S. (2010). Evaluation of aquifer heterogeneity effects on river flow loss using a transition probability framework. *Water Resources Research*, *46*, W01506. https://doi.org/10.1029/2009WR007903

Frei, S., Knorr, K. H., Peiffer, S., & Fleckenstein, J. H. (2012). Surface micro-topography causes hot spots of biogeochemical activity in wetland systems: A virtual modeling experiment. *Journal of Geophysical Research*, *117*, G00N12. https://doi.org/10.1029/2012JG002012

Gomez-Velez, J. D., Harvey, J., Cardenas, M. B., & Kiel, B. (2015). Denitrification in the Mississippi River network controlled by flow through river bedforms. *Nature Geoscience*, *8*(12), 941–U975. https://doi.org/10.1038/ngeo2567

Gomez-Velez, J. D., Krause, S., & Wilson, J. L. (2014). Effect of low-permeability layers on spatial patterns of hyporheic exchange and groundwater upwelling. *Water Resources Research*, *50*, 5196–5215. https://doi.org/10.1002/2013WR015054

Gu, C., Hornberger, G. M., Mills, A. L., Herman, J. S., & Flewelling, S. A. (2007). Nitrate reduction in streambed sediments: Effects of flow and biogeochemical kinetics. *Water Resources Research*, *43*, W12413. https://doi.org/10.1029/2007WR006027

Guin, A., & Ritzi, R. W. (2008). Studying the effect of correlation and finite-domain size on spatial continuity of permeable sediments. *Geophysical Research Letters*, *35*, L10402. https://doi.org/10.1029/2007GL032717

Harter, T. (2005). Finite-size scaling analysis of percolation in three-dimensional correlated binary Markov chain random fields. *Physical Review E*, *72*(2), 026120. https://doi.org/10.1103/PhysRevE.72.026120

Harbaugh, A. W., & McDonald, M. G. (1996). Programmer's Documentation for MODFLOW-96, an update to the U.S. Geological Survey Modular Finite-Difference Ground-Water Flow Model. U.S. Geological Survey Open-File Report 96-486.

Harvey, J. W., Bohlke, J. K., Voytek, M. A., Scott, D., & Tobias, C. R. (2013). Hyporheic zone denitrification: Controls on effective reaction depth and contribution to whole-stream mass balance. *Water Resources Research*, *49*, 6298–6316. https://doi.org/10.1002/wrcr.20492

Hedin, L. O., von Fischer, J. C., Ostrom, N. E., Kennedy, B. P., Brown, M. G., & Robertson, G. P. (1998). Thermodynamic constraints on nitrogen transformations and other biogeochemical processes at soil-stream interfaces. *Ecology*, *79*(2), 684–703. https://doi.org/10.2307/176963

Hester, E. T., Young, K. I., & Widdowson, M. A. (2014). Controls on mixing-dependent denitrification in hyporheic zones induced by riverbed dunes: A steady state modeling study. *Water Resources Research*, *50*, 9048–9066. https://doi.org/10.1002/2014WR015424

Hunter, K. S., Wang, Y., & Van Cappellen, P. (1998). Kinetic modeling of microbially-driven redox chemistry of subsurface environments: Coupling transport, microbial metabolism and geochemistry. *Journal of Hydrology*, *209*(1-4), 53–80. https://doi.org/10.1016/S0022-1694(98)00157-7

Kennedy, C. D., Genereux, P. D., Corbett, D. R., & Mitasova, H. (2009). Spatial and temporal dynamics of coupled groundwater and nitrogen fluxes through a streambed in an agricultural watershed. *Water Resources Research*, *45*, W09401. https://doi.org/10.1029/2008WR007397

Kessler, A. J., Glud, R. N., Cardenas, M. B., Larsen, M., Bourke, M. F., & Cook, P. L. M. (2012). Quantifying denitrification in rippled permeable sands through combined flume experiments and modeling. *Limnology and Oceanography*, *57*(4), 1217–1232. https://doi.org/10.4319/lo.2012.57.4.1217

Korom, S. F. (1992). Natural denitrification in the saturated zone: A review. *Water Resources Research*, *28*(6), 1657–1668. https://doi.org/10.1029/92WR00252

Krause, S., Tecklenburg, C., Munz, M., & Naden, E. (2013). Streambed nitrogen cycling beyond the hyporheic zone: Flow controls on horizontal patterns and depth distribution of nitrate and dissolved oxygen in the upwelling groundwater of a lowland river. *Journal of Geophysical Research: Biogeosciences*, *118*, 54–67. https://doi.org/10.1029/2012JG002122

Laube, G., Schmidt, C., & Fleckenstein, J. H. (2018). The systematic effect of streambed conductivity heterogeneity on hyporheic flux and residence time. *Advances in Water Resources*, *122*, 60–69. https://doi.org/10.1016/j.advwatres.2018.10.003

Lewandowski, J., & Nutzmann, G. (2010). Nutrient retention and release in a floodplain's aquifer and in the hyporheic zone of a lowland river. *Ecological Engineering*, *36*(9), 1156–1166. https://doi.org/10.1016/j.ecoleng.2010.01.005

Malard, F., & Hervant, F. (1999). Oxygen supply and the adaptations of animals in groundwater. *Freshwater Biology*, *41*(1), 1–30. https://doi.org/10.1046/j.1365-2427.1999.00379.x

Marzadri, A., Tonina, D., & Bellin, A. (2012). Morphodynamic controls on redox conditions and on nitrogen dynamics within the hyporheic zone: Application to gravel bed rivers with alternate-bar morphology. *Journal of Geophysical Research*, *117*, G00N10. https://doi.org/10.1029/2012JG001966

Nixon, S. W. (1995). Coastal marine eutrophication: A definition, social causes, and future concerns. *Ophelia*, *41*(1), 199–219. https://doi.org/10.1080/00785236.1995.10422044

Peterson, E. W., & Hayden, K. M. (2018). Transport and fate of nitrate in the streambed of a low-gradient stream. *Hydrology*, *5*(4), 55. https://doi.org/10.3390/hydrology5040055

Pollock, D. W. (2012). User guide for MODPATH version 6—A particle-tracking model for MODFLOW: U.S. Geological Survey techniques and methods 6–A41, 58 p.

Pryshlak, T. T., Sawyer, A. H., Stonedahl, S. H., & Soltanian, M. R. (2015). Multiscale hyporheic exchange through strongly heterogeneous sediments. *Water Resources Research*, *51*, 9127–9140. https://doi.org/10.1002/2015WR017293

Puckett, L. J., Cowdery, T. K., McMahon, P. B., Tornes, L. H., & Stoner, J. D. (2002). Using chemical, hydrologic, and age dating analysis to delineate redox processes and flow paths in the riparian zone of a glacial outwash aquifer-stream system. *Water Resources Research*, *38*(8), 1134. https://doi.org/10.1029/2001WR000396

Puckett, L. J., Zamora, C., Essaid, H., Wilson, J. T., Johnson, H. M., Brayton, M. J., & Vogel, J. R. (2008). Transport and fate of nitrate at the ground-water/surface-water interface. *Journal of Environmental Quality*, *37*(3), 1034–1050. https://doi.org/10.2134/jeq2006.0550

Ritzi, R. W., Dai, Z., Dominic, D. F., & Rubin, Y. N. (2004). Spatial correlation of permeability in cross-stratified sediment with hierarchical architecture. *Water Resources Research*, *40*, W03513. https://doi.org/10.1029/2003WR002420

Sawyer, A. H. (2015). Enhanced removal of groundwater-borne nitrate in heterogeneous aquatic sediments. *Geophysical Research Letters*, *42*, 403–410. https://doi.org/10.1002/2014GL062234

Seitzinger, S. P., Styles, R. V., Boyer, E. W., Alexander, R. B., Billen, G., Howarth, R. W., et al. (2002). Nitrogen retention in rivers: Model development and application to watersheds in the northeastern U.S.A. *Biogeochemistry*, *57*(1), 199–237. https://doi.org/10.1023/a:1015745629794

Shampine, L. F., & Reichelt, M. W. (1997). The MATLAB ODE Suite. *SIAM Journal on Scientific Computing*, *18*(1), 1–22. https://doi.org/10.1137/S1064827594276424

Soltanian, M. R., Ritzi, R., Dai, Z., Huang, C., & Dominic, D. (2015). Transport of kinetically sorbing solutes in heterogeneous sediments with multimodal conductivity and hierarchical organization across scales. *Stochastic environmental research and risk assessment*, *29*(3), 709–726. https://doi.org/10.1007/s00477-014-0922-3

Soltanian, M. R., Ritzi, R. W., Huang, C. C., & Dai, Z. (2015a). Relating reactive solute transport to hierarchical and multiscale sedimentary architecture in a Lagrangian-based transport model: 1. Time-dependent effective retardation factor. *Water Resources Research*, *51*, 1586–1600. https://doi.org/10.1002/2014WR016353

Soltanian, M. R., Ritzi, R. W., Huang, C. C., & Dai, Z. (2015b). Relating reactive solute transport to hierarchical and multiscale sedimentary architecture in a Lagrangian-based transport model: 2. Particle displacement variance. *Water Resources Research*, *51*, 1601–1618. https://doi.org/10.1002/2014WR016354

Soltanian, M. R., Sun, A., & Dai, Z. (2017). Reactive transport in the complex heterogeneous alluvial aquifer of Fortymile Wash, Nevada. *Chemosphere*, *179*, 379–386. https://doi.org/10.1016/j.chemosphere.2017.03.136

Starr, R. C., & Gillham, R. W. (1993). Denitrification and organic carbon availability in two aquifers. *Ground Water*, *31*(6), 934–947. https://doi.org/10.1111/j.1745-6584.1993.tb00867.x

Stelzer, R. S., Bartsch, L. A., Richardson, W. B., & Strauss, E. A. (2011). The dark side of the hyporheic zone: Depth profiles of nitrogen and its processing in stream sediments. *Freshwater Biology*, *56*(10), 2021–2033. https://doi.org/10.1111/j.1365-2427.2011.02632.x

Stelzer, R. S., Scott, J. T., Bartsch, L. A., & Parr, T. B. (2014). Particulate organic matter quality influences nitrate retention and denitrification in stream sediments: Evidence from a carbon burial experiment. *Biogeochemistry*, *119*(1-3), 387–402. https://doi.org/10.1007/s10533-014-9975-0

Trauth, N., & Fleckenstein, J. H. (2017). Single discharge events increase reactive efficiency of the hyporheic zone. *Water Resources Research*, *53*, 779–798. https://doi.org/10.1002/2016WR019488

Trauth, N., Schmidt, C., Vieweg, M., Maier, U., & Fleckenstein, J. H. (2014). Hyporheic transport and biogeochemical reactions in pool-riffle systems under varying ambient groundwater flow conditions. *Journal of Geophysical Research: Biogeosciences*, *119*, 910–928. https://doi.org/10.1002/2013JG002586

Triska, F. J., Duff, J. H., & Avanzino, R. J. (1993). Patterns of hydrological exchange and nutrient transformation in the hyporheic zone of a gravel-bottom stream: Examining terrestrial-aquatic linkages. *Freshwater Biology*, *29*(2), 259–274. https://doi.org/10.1111/j.1365-2427.1993.tb00762.x

Vitousek, P. M., Aber, J. D., Howarth, R. W., Likens, G. E., Matson, P. A., Schindler, D. W., et al. (1997). Human alteration of the global nitrogen cycle: Sources and consequences. *Ecological Applications*, *7*(3), 737–750. https://doi.org/10.2307/2269431

Warner, T. J., Royer, T. V., Tank, J. L., Griffiths, N. A., Rosi-marshall, E. J., & Whiles, M. R. (2009). Dissolved organic carbon in streams from artificially drained and intensively farmed watersheds in Indiana, USA. *Biogeochemistry*, *95*(2-3), 295–307. https://doi.org/10.1007/s10533-009-9337-5

Weissmann, G. S., Carle, S. F., & Fogg, G. E. (1999). Three-dimensional hydrofacies modeling based on soil surveys and transition probability geostatistics. *Water Resources Research*, *35*(6), 1761–1770. https://doi.org/10.1029/1999WR900048

Weissmann, G. S., & Fogg, G. E. (1999). Multi-scale alluvial fan heterogeneity modeled with transition probability geostatistics in a sequence stratigraphic framework. *Journal of Hydrology*, *226*(1-2), 48–65. https://doi.org/10.1016/S0022-1694(99)00160-2

Zarnetske, J. P., Haggerty, R., Wondzell, S. M., & Baker, M. A. (2011a). Dynamics of nitrate production and removal as a function of residence time in the hyporheic zone. *Journal of Geophysical Research*, *116*, G01025. https://doi.org/10.1029/2010JG001356

Zarnetske, J. P., Haggerty, R., Wondzell, S. M., & Baker, M. A. (2011b). Labile dissolved organic carbon supply limits hyporheic denitrification. *Journal of Geophysical Research*, *116*, G04036. https://doi.org/10.1029/2011JG001730

Zhou, Y., Ritzi, R. W., Soltanian, M. R., & Dominic, D. F. (2014). The influence of streambed heterogeneity on hyporheic flow in gravelly rivers. *Groundwater*, *52*(2), 206–216. https://doi.org/10.1111/gwat.12048

Zolezzi, G., & Seminara, G. (2001). Downstream and upstream influence in river meandering. Part 1. General theory and application to overdeepening. *Journal of Fluid Mechanics*, *438*, 183–211.

Erratum

In the originally published version of this article, Figures 1, 2, and 3 were published with incorrect labeling. The figure order is now correct, and this version may be considered the authoritative version of record.